Imaging transition metals in the brain

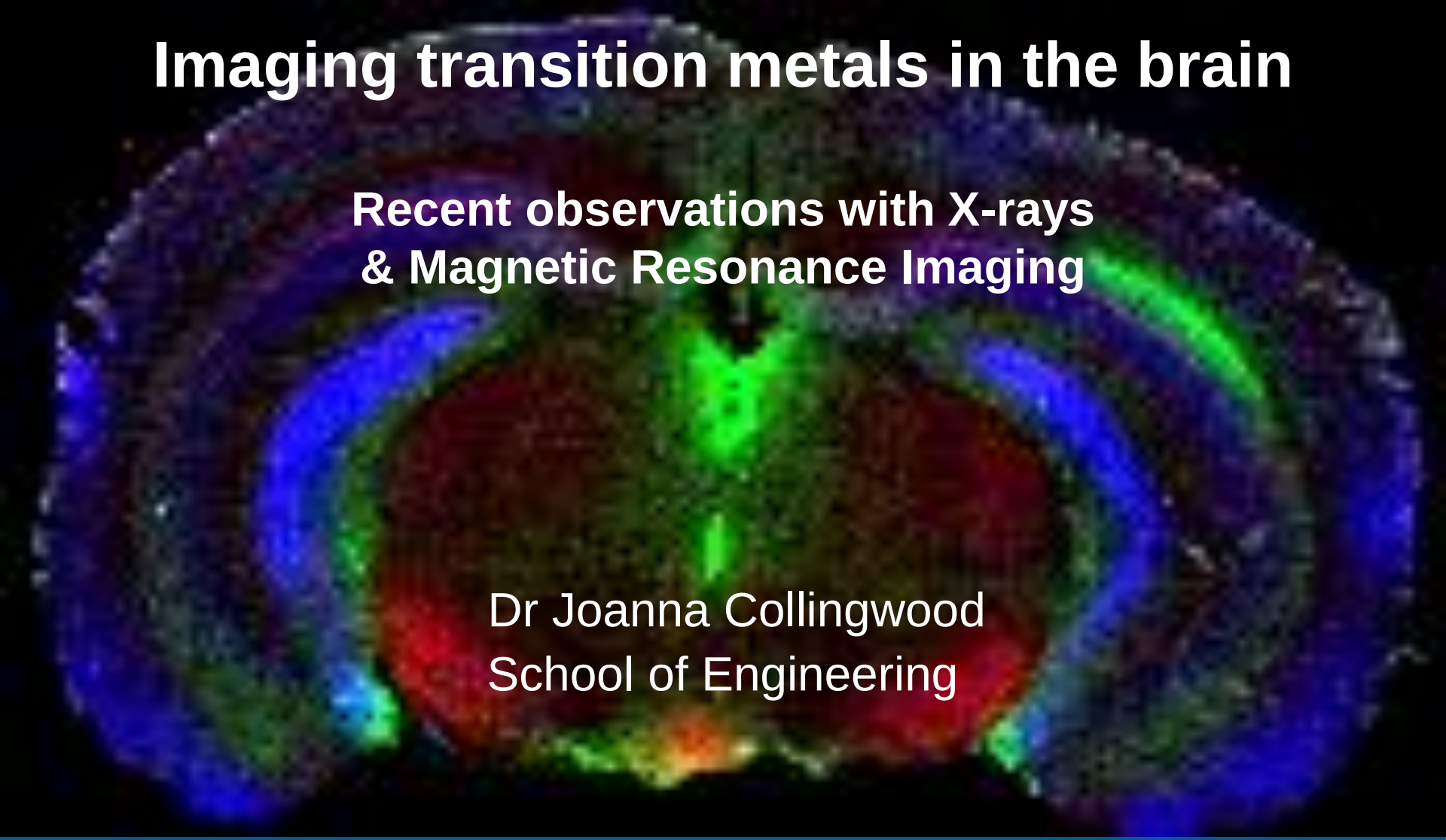

Recent observations with X-rays & Magnetic Resonance Imaging

Dr Joanna Collingwood
School of Engineering

THE UNIVERSITY OF WARWICK

Dysregulation of iron in the human brain…

- Alzheimer's disease
- Parkinson's disease
- Huntington's disease
- Multiple sclerosis
- NBIA / PKAN
- Neuroferritinopathy
- Motor neurone disease (ALS)
- Friedreich's ataxia
- Aceruloplasminaemia
- Progressive supranuclear palsy
- Down syndrome
- Multiple System Atrophy
- HIV-associated dementia

Adapted from Thompson et al, 2001 Brain Research Bulletin, 55, 155-164

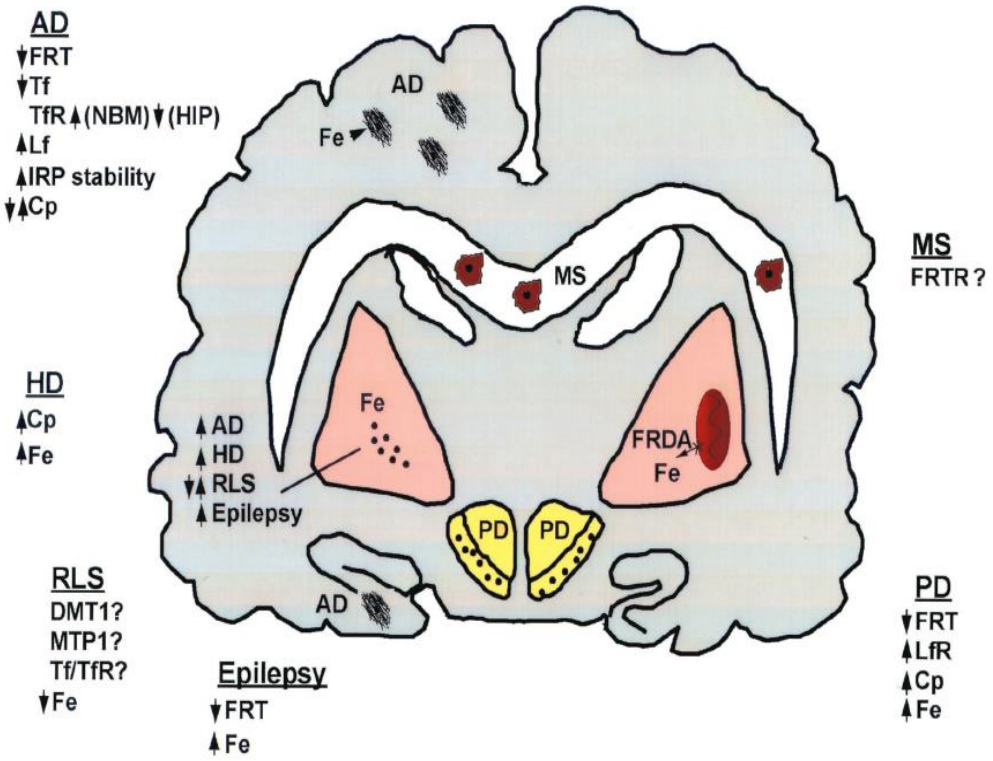

TRANSITION METALS IN NEURODEGENERATION

Neurodegenerative disorders with possible metal-associated pathology (modified from Crichton 2006)

Disorder	Implicated Metal	Implicated metalloproteins or enzymes
Alzheimer's disease	Iron, aluminium, copper, zinc	Aβ, APP
Parkinson's disease	Iron, manganese	α-synuclein, neuromelanin, lactoferrin, ferritin, melanotransferrin, ceruloplasmin, divalent cation transporter
CJD	Iron, copper	Prion protein
Friedreich's ataxia	Copper, zinc deficiency	Frataxin, aconitase, mitochondrial proteins
Multiple sclerosis	Iron	Unknown
Wilson's disease	Copper	Ceruloplasmin deficiency, Wilson's protein
NBIA	Iron	Vitamin B5 metabolism (PANK2)
Huntington's disease	Iron, calcium	Huntingtin
Aceruloplasminaemia	Iron	Ceruoplasmin

TRANSITION METALS IN NEURODEGENERATION

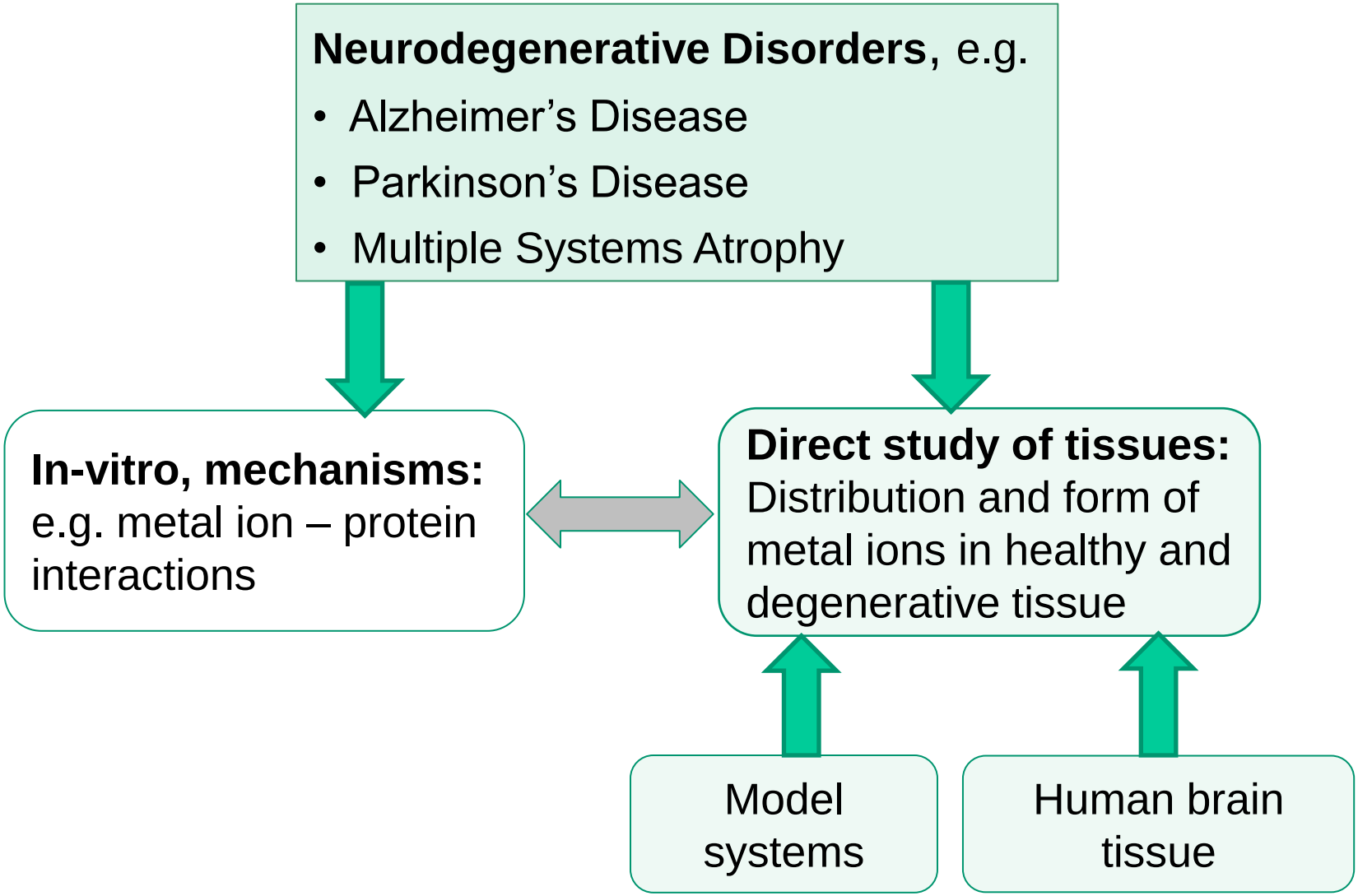

TRADITIONAL STUDIES OF IRON IN THE BRAIN

Staining and light microscopy

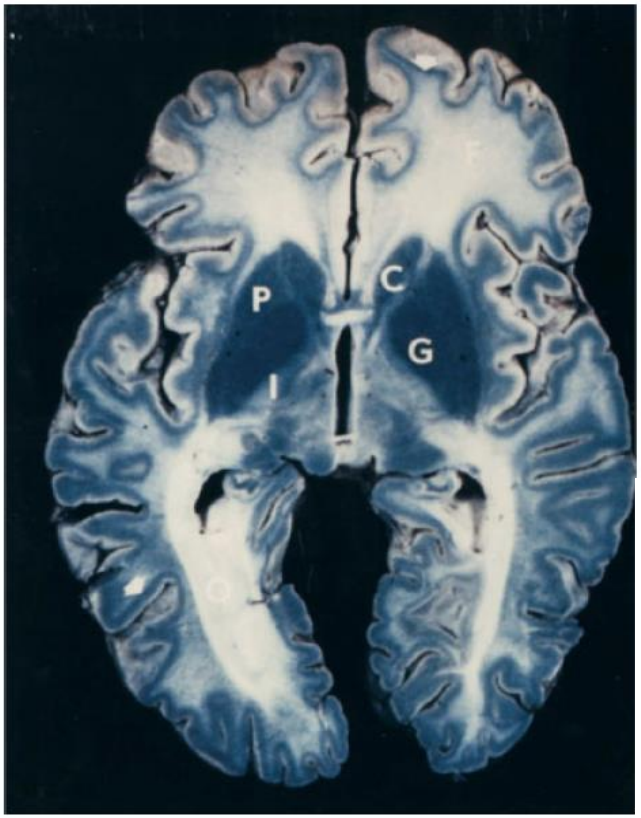

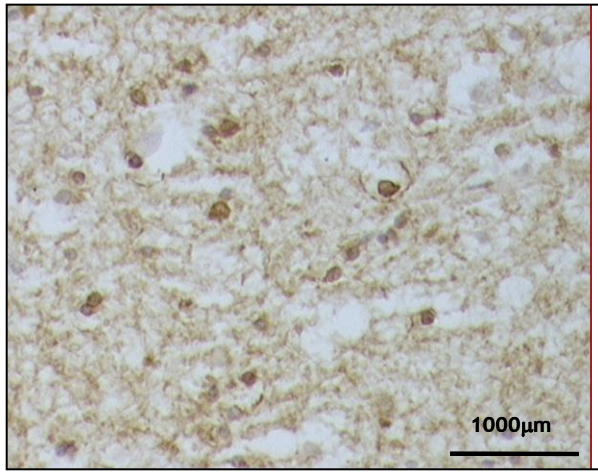

Light microscopy image of human brain tissue from an Alzheimer's case, antibody stained for ferritin (brown).

Example of Perls stain in normal brain of 44 year old man, after Drayer et al, 1986, Am J Roentgenol.

Electron microprobe analysis: Iron in Parkinson's disease

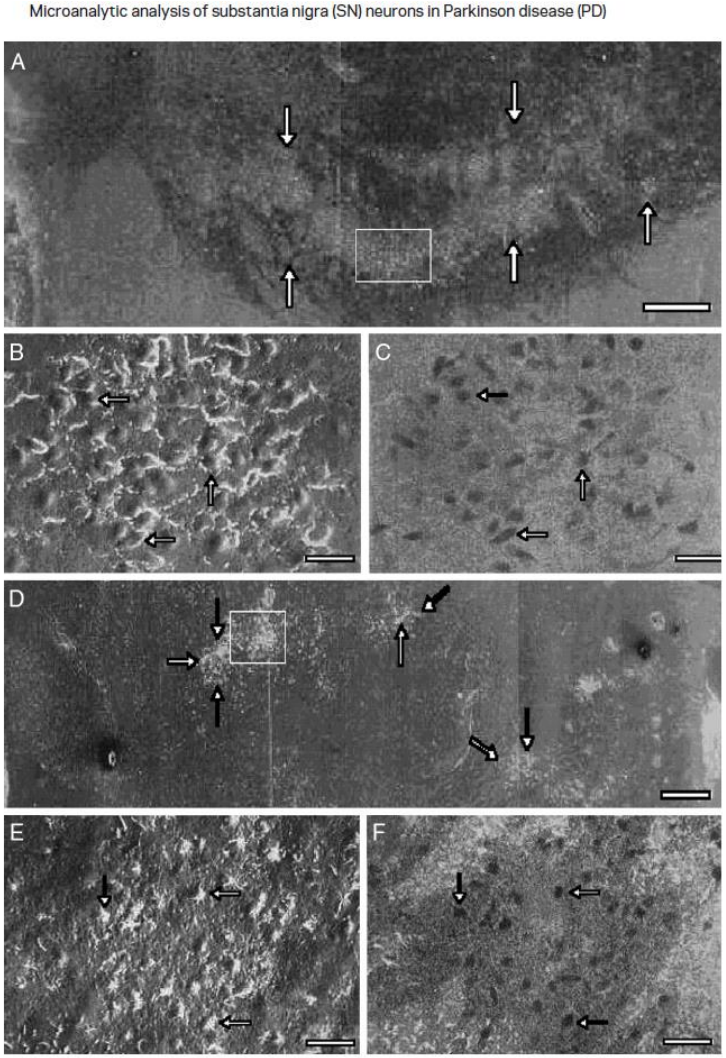

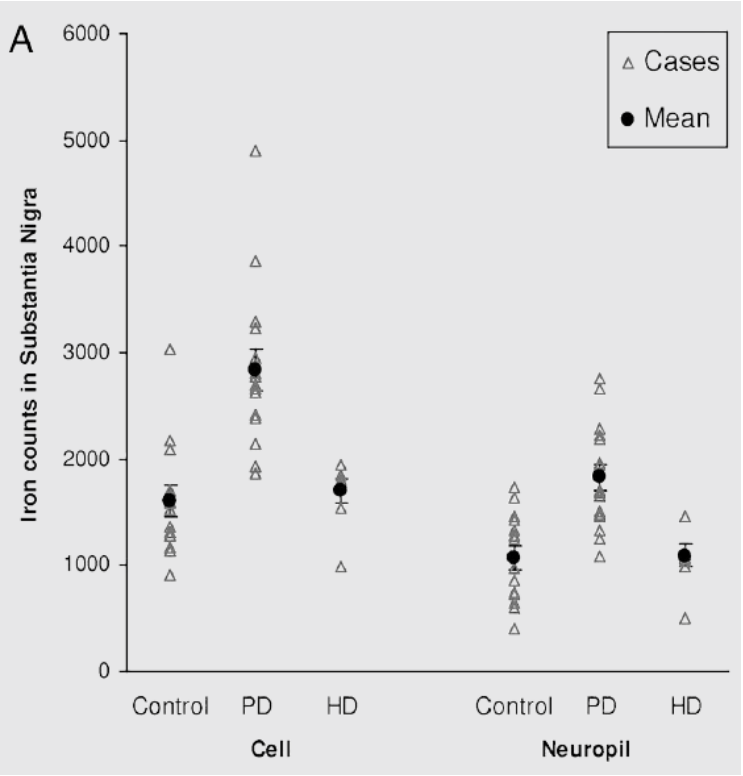

Raised intraneuronal iron in single defined substantia nigra neurons in PD (***p* < 0.0001**) but not in other movement disorders such as Huntington disease.

Findings unrelated to the density of remaining neurons.

A.E. Oakley, J.F. Collingwood, J. Dobson, G. Love, H R Perrot, J.A. Edwardson, C.M. Morris, Neurology, 2007, 68, 1825.

Synchrotron microfocus X-Ray Fluorescence (µXRF)

Diamond Light Source, I18 beamline, Oxfordshire, UK

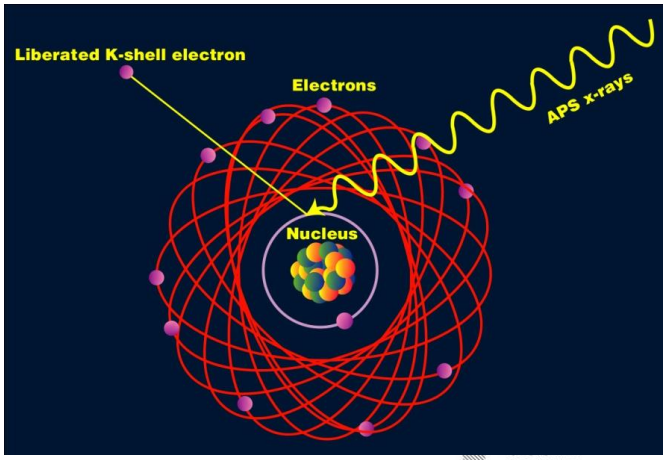

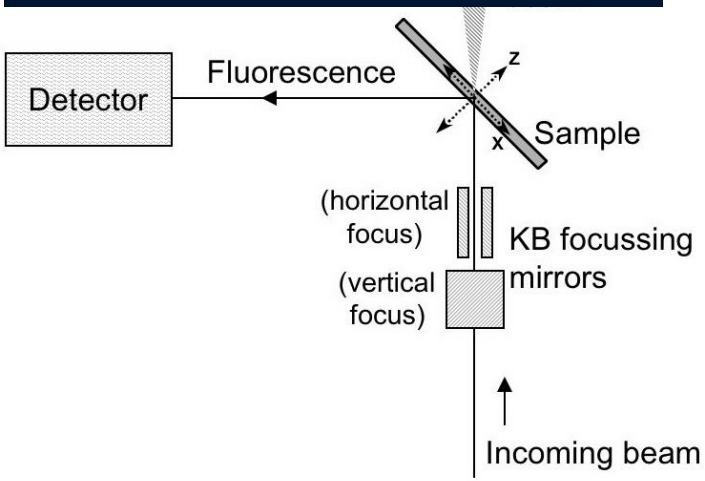

Analytica Chimica Acta, 195 (1987) 153—162
Elsevier Science Publishers B.V., Amsterdam — Printed in The Netherlands

BULK AND MICROPROBE ANALYSIS FOR TRACE ELEMENTS WITH SYNCHROTRON RADIATION

W. J. M. LENGLET, R. D. VIS, F. VAN LANGEVELDE and H. VERHEUL

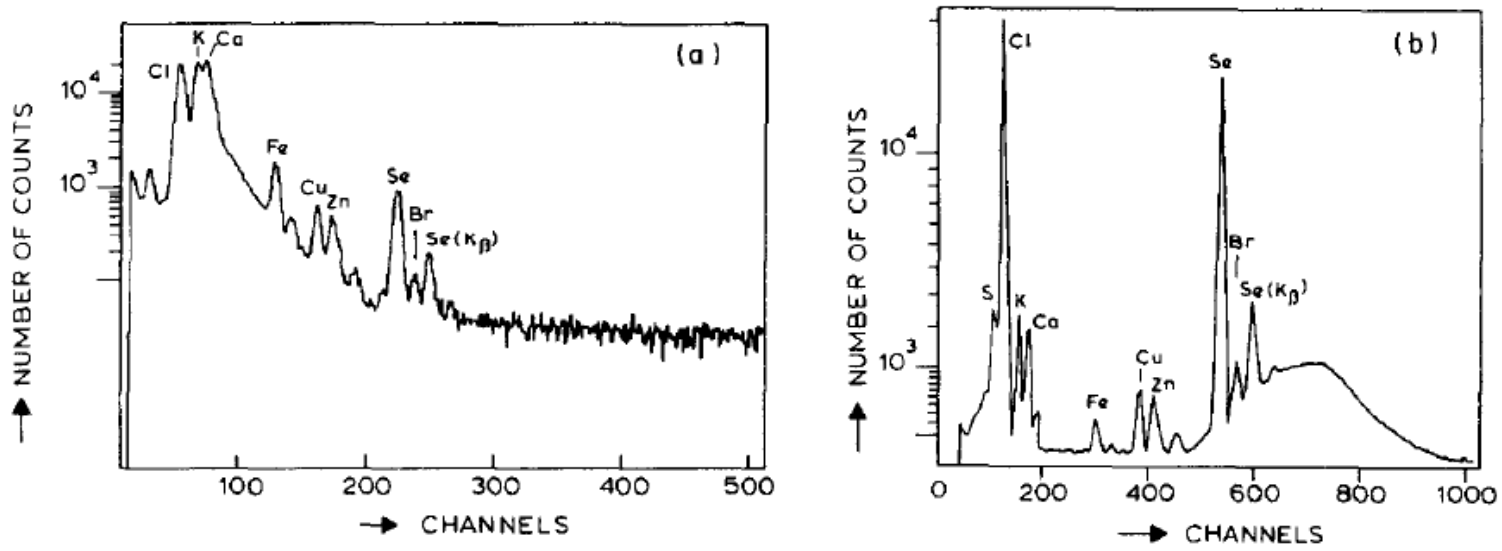

Fig. 3. Typical x-ray spectra of blood serum: (a) excited with protons of 2.5 MeV; (b) excited with synchrotron radiation of 15 keV. The characteristic lines of the relevant trace elements are indicated.

µXRF MAPPING OF TRACE METALS

Raster sample in x-y plane to obtain map of relative intensity

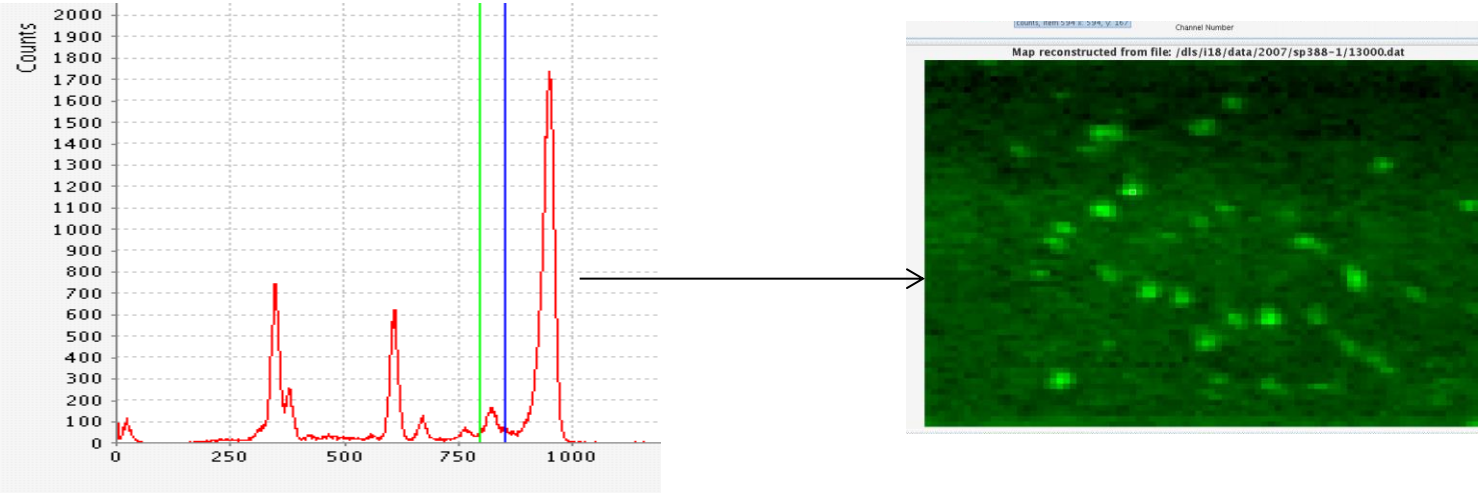

Fitting of peaks (e.g. in PyMCA) to avoid ‘phantom’ elements

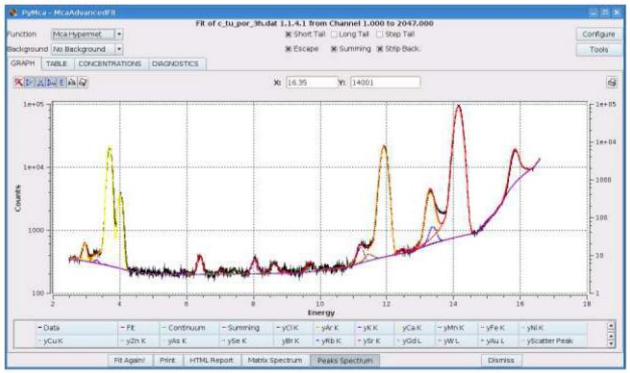

TRACE METALS IN THE RETINA

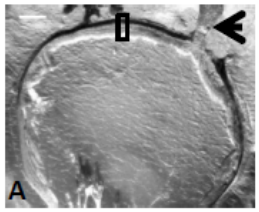

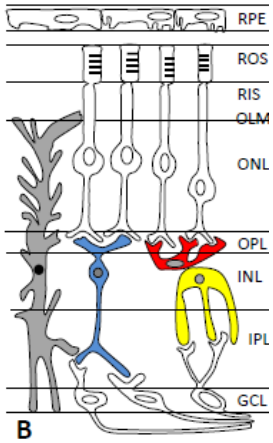

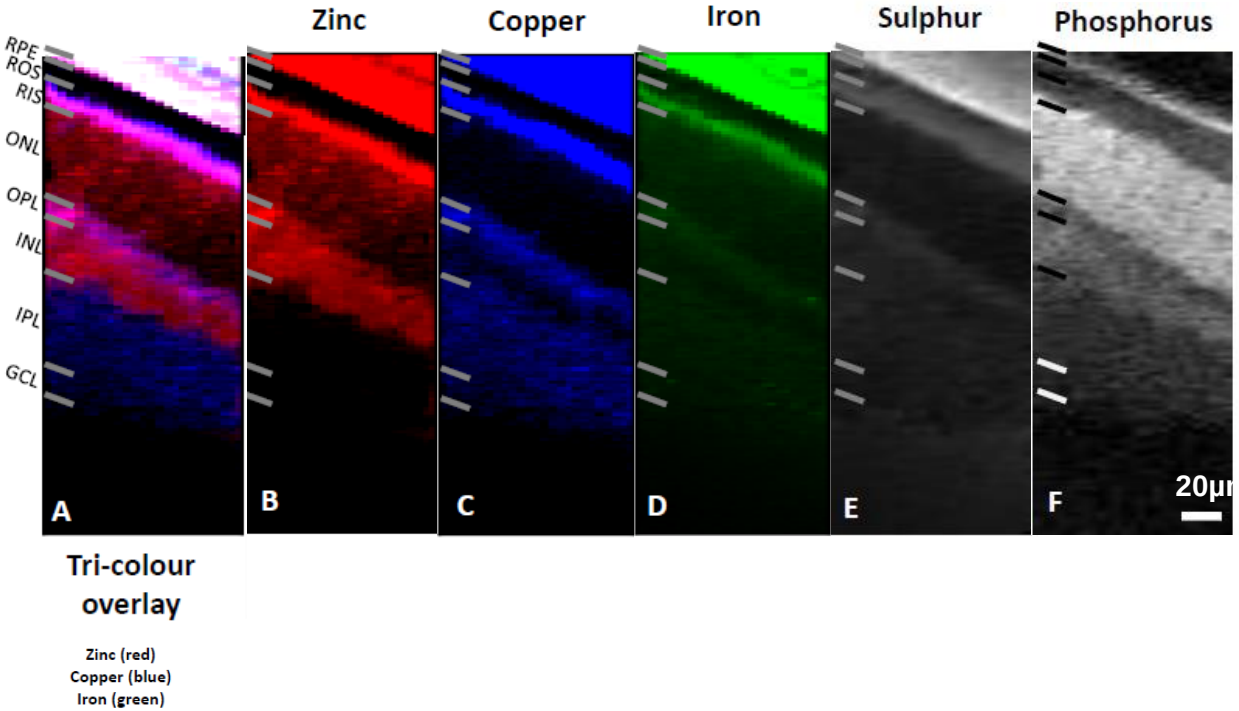

Demonstrated at I18 that it is possible to localise the distribution of total iron, zinc and copper in retinal sections

Currently in the process of comparing retinas from a diabetes-like rat model versus age-matched animals.

Ugarte M., Grime G.W., Lord G., Geraki K., Collingwood J.F., Finnegan M.E., et al, Metallomics, 2012, DOI:10.1039/C2MT20157G

SPHERULITES IN ALZHEIMER'S HIPPOCAMPUS

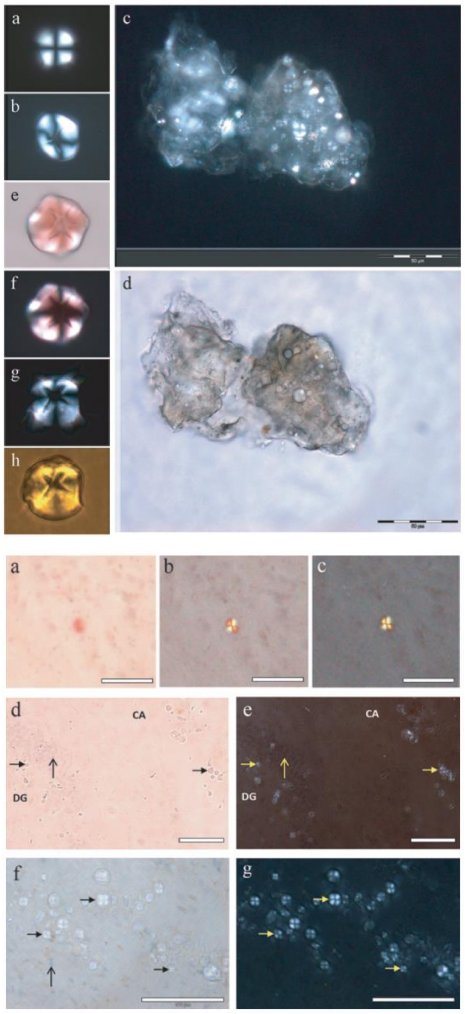

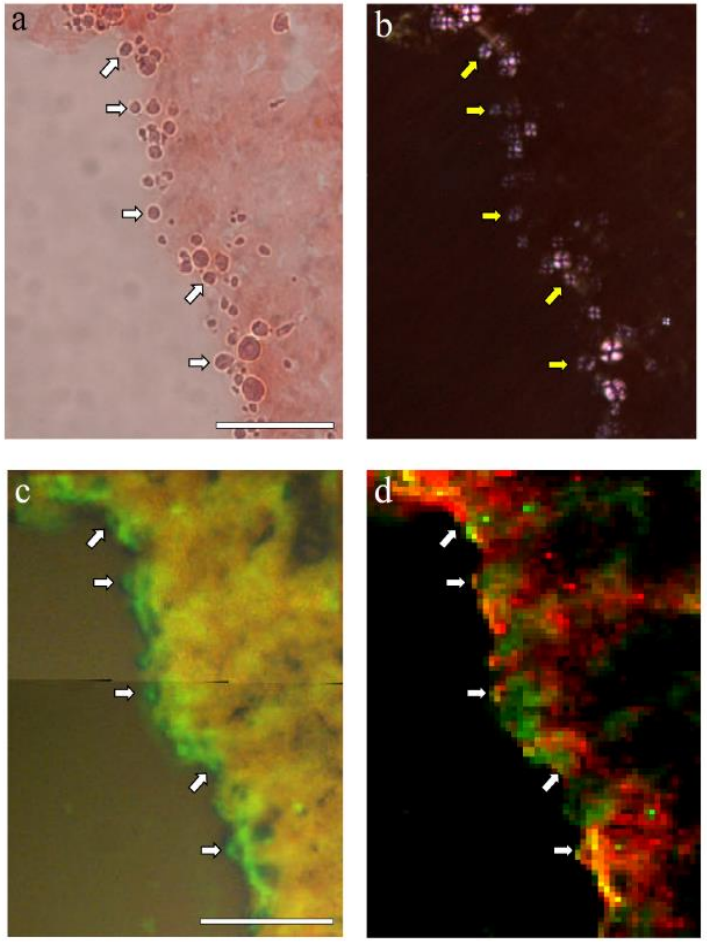

C. Exley, E. House, J.F. Collingwood, M.R. Davidson, D. Cannon, A.M. Donald (2010) 'Spherulites of Aß42 in vitro and in Alzheimer's disease' *Journal of Alzheimer's Disease* 20 (4), p 1159 - 1165 (1387-2877)

µXRF and µXANES OF ALZHEIMER'S DISEASE TISSUE

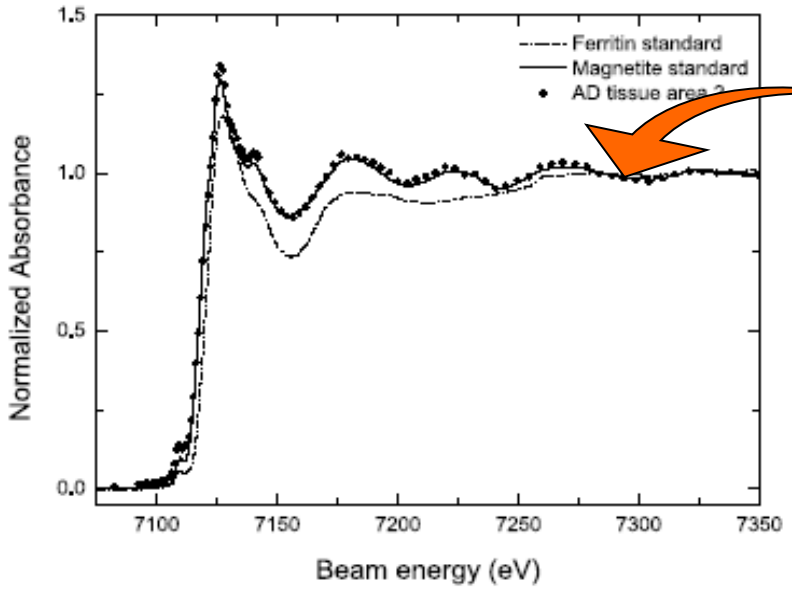

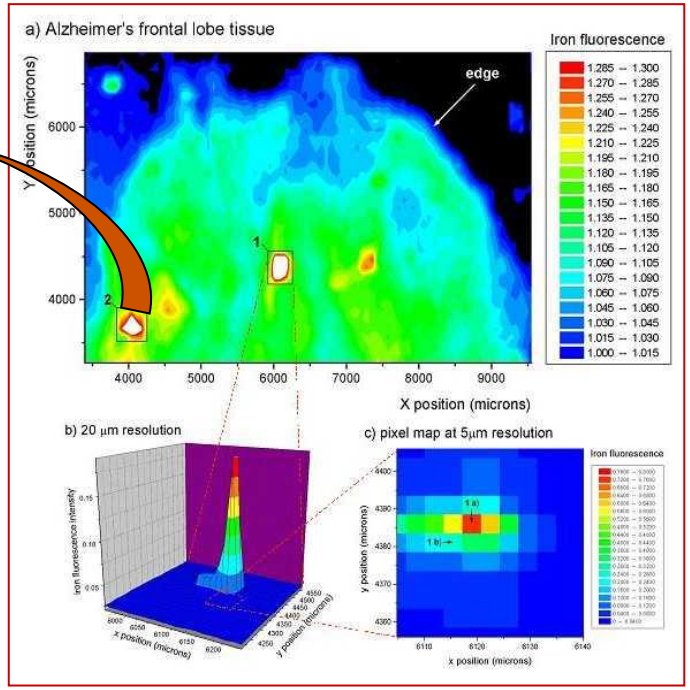

Superior frontal gyrus tissue: senile-plaque-rich as confirmed by staining in adjacent section.

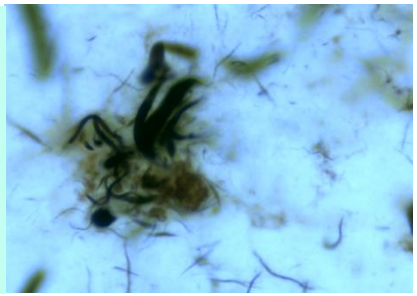

MRCAT, 10-ID-B, APS, Argonne

Table 1
A selection of results from linear-combination fits of the XANES region that used measured standards from ferritin, magnetite, hematite, metallic iron, hemoglobin, and maghemite

Scan area	Ferritin (%)	Magnetite (%)	Fitting parameter (χ^2)
1a	0	100	0.61
1b	21	79	0.24
2	0	100	0.88

J F Collingwood et al, J Alzheimer's Dis. 2005**, 7** 267-272

TRANSGENIC MODEL OF ALZHEIMER'S DISEASE

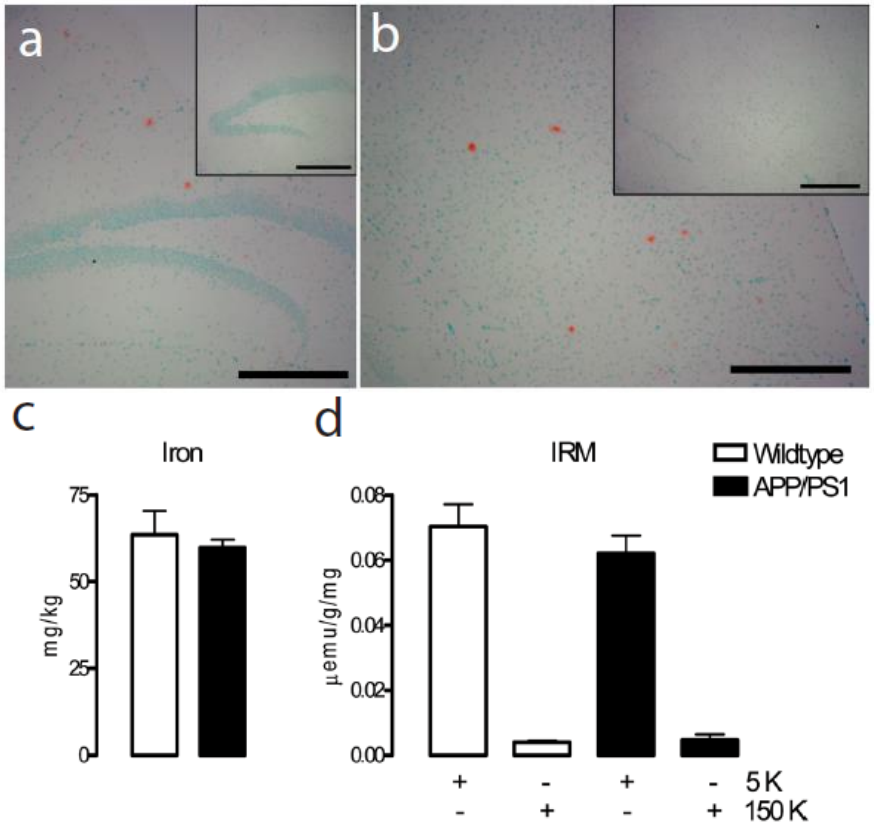

The total iron concentration and IRM of a single brain hemisphere is not altered by the amyloid deposition associated with 8-9 month old AβPP/PS1 tg mice

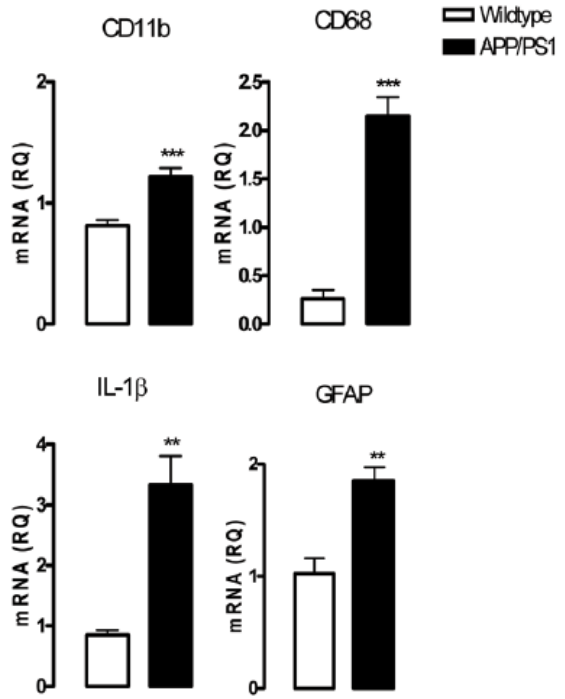

Modest amyloid deposition is associated with an increase in markers of microglial and astrocytic activation and oxidative stress

J.J. Gallagher, M.E. Finnegan, B. Grehan, J. Dobson, J.F. Collingwood & M.A. Lynch, J. Alzheimer's Disease **28** (2012) 147–161

TRANSGENIC MODEL OF ALZHEIMER'S DISEASE

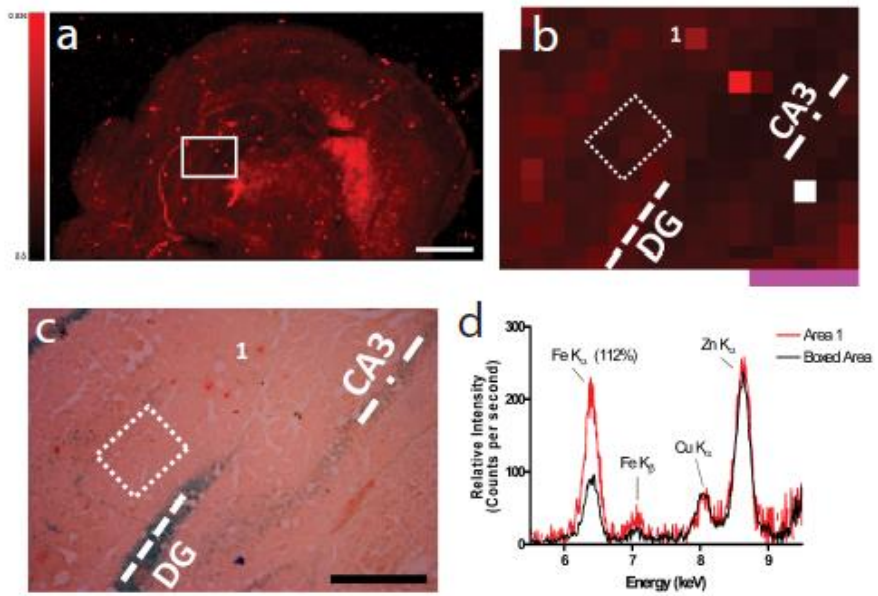

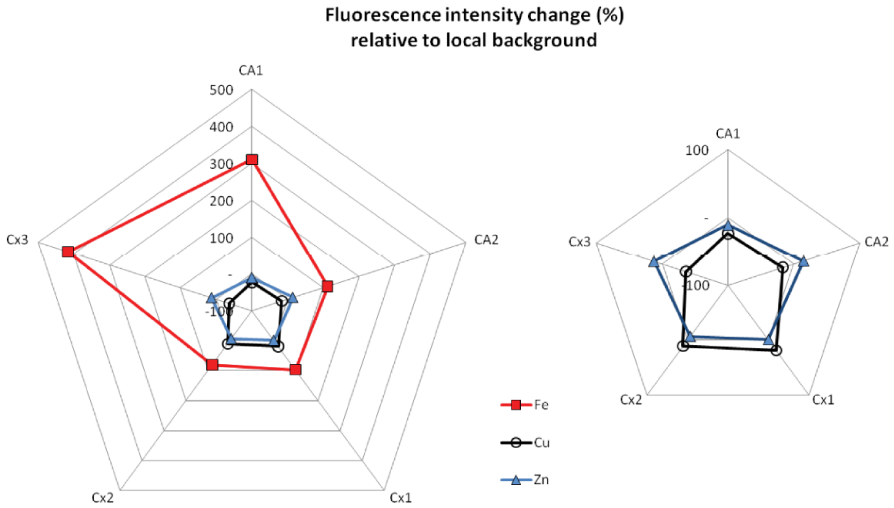

Iron levels are increased in tissue associated with Aβ-containing plaques

J.J. Gallagher, M.E. Finnegan, B. Grehan, J. Dobson, J.F. Collingwood & M.A. Lynch, J. Alzheimer's Disease **28** (2012) 147–161

TRANSGENIC MODEL OF ALZHEIMER'S DISEASE

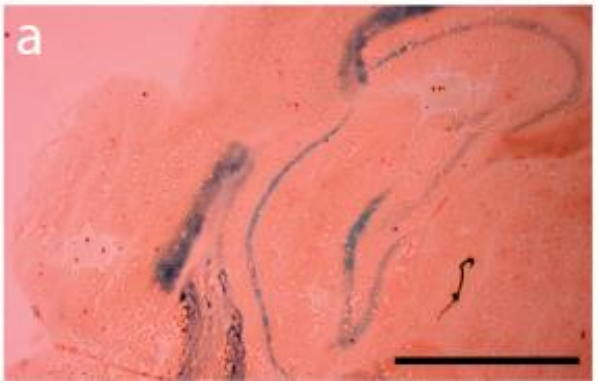

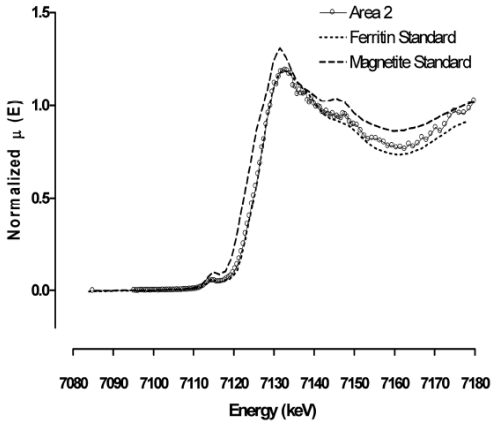

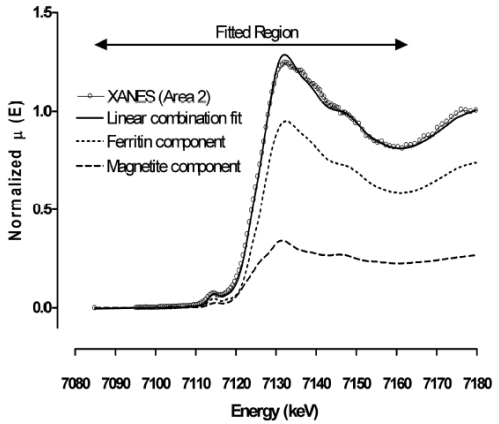

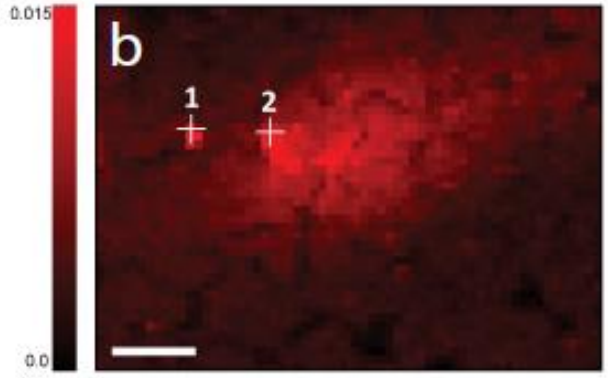

XANES spectra linear-combination fits

	Magnetite	Ferritin	Fitting Parameter (χ^2)
Area 1	16 %	84 %	0.036
Area 2	26 %	74 %	0.044

Mixed-valence iron oxides are present in brain tissue associated with high iron deposition

J.J. Gallagher, M.E. Finnegan, B. Grehan, J. Dobson, J.F. Collingwood & M.A. Lynch, J. Alzheimer's Disease **28** (2012) 147–161

SUMMARY

- Findings from the APP/PS1 transgenic mouse model of Alzheimer's disease support the contention that, in addition to glial activation and oxidative stress, iron dysregulation is an early event in AD pathology.

J.J. Gallagher, M.E. Finnegan, B. Grehan, J. Dobson, J.F. Collingwood & M.A. Lynch, J. Alzheimer's Disease **28** (2012) 147–161

Detecting iron with MRI

MRI to quantify iron in tissues

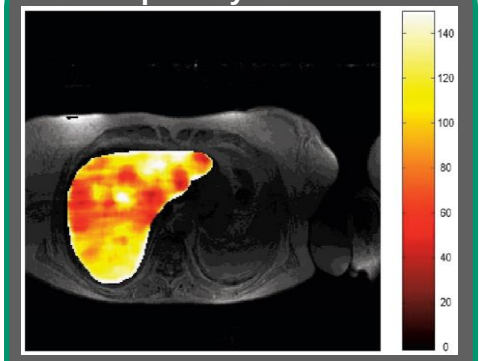

Carneiro et al, Liver Iron Concentration Evaluated by Two Magnetic Methods: Magnetic Resonance Imaging and Magnetic Susceptometry, Magnetic Resonance in Medicine **54** (2005) 122

Altered regional brain iron concentrations in PD

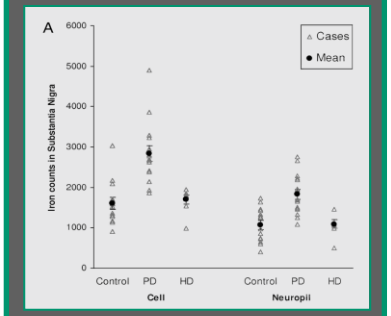

Oakley et al, Individual dopaminergic neurons show raised iron levels in Parkinson disease, Neurology **68** (2007) 1820

Potential of MRI to detect brain iron changes in Parkinson's patients

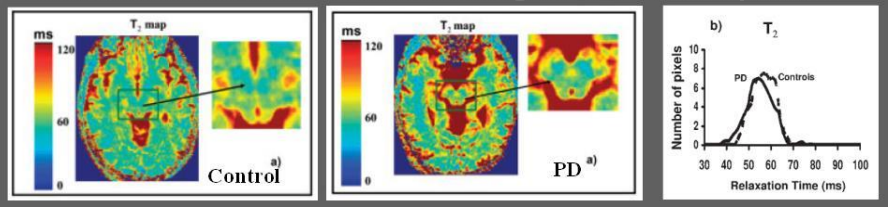

Michaeli et al, Assessment of Brain Iron and Neuronal Integrity in Patients with Parkinson's Disease Using Novel MRI Contrasts, Movement Disorders **22** (2007) 334

- Liver iron measurement with MRI successfully demonstrated by others, e.g. St Pierre. (Used supporting biopsy evidence.)
- Biopsy route not so popular for human brain... Primarily dependent on post-mortem tissues for study.
- House et al, MRM (2007): threshold iron concentration of 55 µg Fe/g wet tissue above which R_2 appears dominated by iron in AD brain tissue.
- **Aim: spatial correlation between relevant MRI parameters (e.g. R_2, R_2*) and iron distribution**

MRI analysis

Bruker 600 MHz (14.1 T) NMR Spectrometer

Bruker 5 mm TXI microimaging cryoprobe

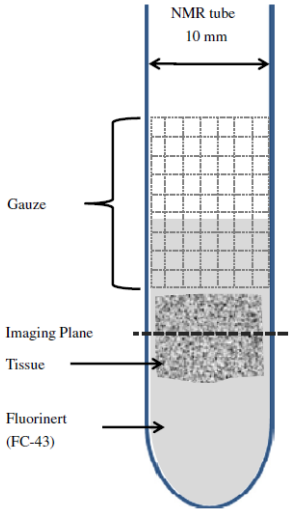

Advanced Magnetic Resonance Imaging and Spectroscopy (AMRIS), McKnight Brain Institute, The University of Florida, Gainesville.

Tissue @ 3°C during measurement

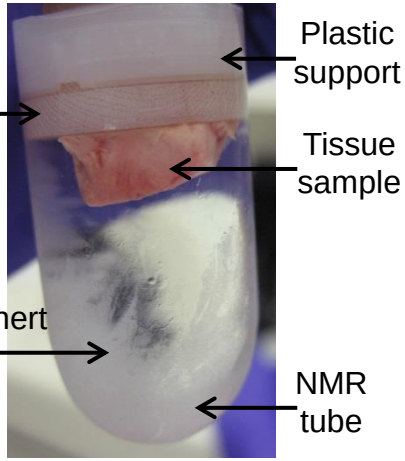

Summary of MRI acquisition parameters for microscopy measurement of R_2^* (multi-gradient-echo), R_2 (multi-spin multi-echo CPMG sequence) and for lower resolution measurement of R_1 (CPMG sequence with variable repetition time T_R).

Parameters	R_2^*	R_2	R_1
Pulse sequence	Multiple gradient echo (MGE)	Multi-spin multi-echo (MSME)	MSME variable T_R (MSME-VTR)
Pulse shape	Gaussian	sinc3	sinc3
FOV (mm)	8×8	8×8	10×10
Matrix size	128×128	128×128	40×40
Spatial resolution	62 μm	62 μm	250 μm
Slice thickness	80 μm	80 μm	250 μm
T_E (ms)	3.70 (minimum)	8.62 (minimum)	9.62
Δ T_E (ms)	6.66	8.62	–
# T_E	18	15	1
T_R (ms)	4500	4000	250 to 4500
# T_R	1	1	8
# Averages	12	12	3
Sequence duration	90 min	100 min	20 min

V. Antharam, J. F. Collingwood, et al. (2012) Neuroimage 59(2): 1249-1260.

SUBSTANTIA NIGRA; Parkinson's disease

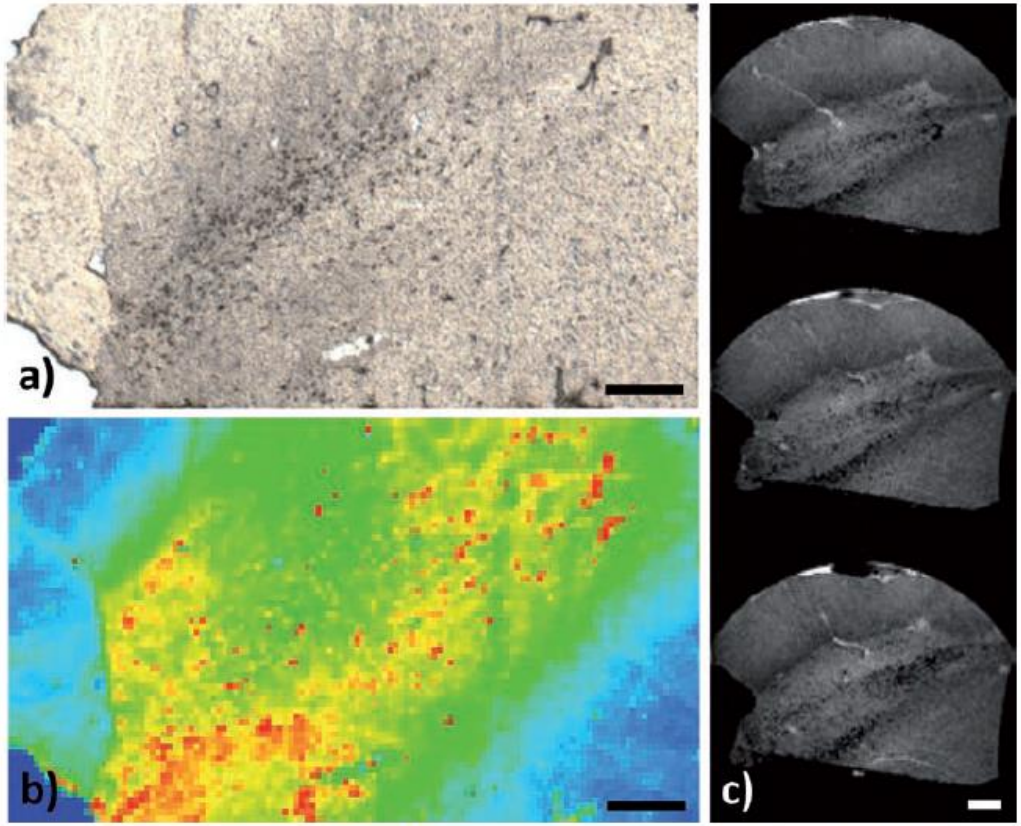

Figure 1 | Interpreting the contribution of iron to MRI signal in the substantia nigra of an elderly case without Parkinson's disease. a, Photograph showing brown deposits of neuromelanin, typically found in dopaminergic neurons (scale bar, 1 mm). **b**, Corresponding X-ray fluorescence map of iron distribution from low (blue) to high (red) concentration (scale bar, 1 mm). **c**, T2* MRI microscopy in original block of unfixed tissue (scale bar, 500 μm). For further details, see ref. 6. Picture credits: J. F. Collingwood (**a**–**c**), University of Warwick; M. R. Davidson (**b**), A. Mikhailova (**a**), J. P. Bullivant (**c**), V. Antharam (**a**, **c**), C. Batich (**c**) and J. Forder (**c**), University of Florida; J. Dobson (**b**), Keele University; and P. D. Quinn (**b**) and J. F. W. Mosselmans (**b**), Diamond Light Source.

Jones R., Nature Outlooks, August 2010
&
Collingwood, J. F. et al. Mov. Dis. 23 (suppl. 1), abstr. S62 (2008)

MRI OF BRAIN IRON IN ALZHEIMER'S DISEASE

- Iron can affect contrast in MRI using certain parameters (e.g. R_2, R_2*)
- Can we obtain direct confirmation of this in human tissue?
- Are there detectable changes in total iron concentration in hippocampus?
- Are 'hotspots' from pathologic iron deposition (e.g. in senile plaques) detectable?

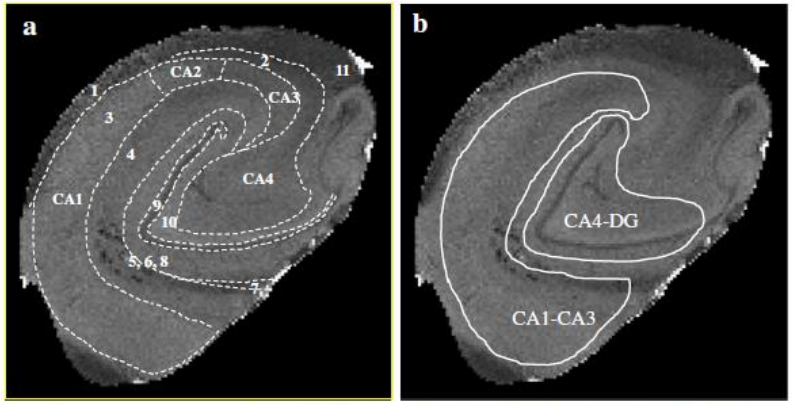

Subfields indicated above
1. Alveus (ALV)
2. Stratum oriens
3. Stratum pyramidale (SP)
4. Stratum radiatum (SR)
5. Stratum lacunosum
6. Stratum moleculare (SM)
7. Hippocampal sulcus
8. Stratum moleculare (SM)
9. Stratum granulosum (SG)
10. Polymorphic layer (PL)
11. Fimbria

CA4-DG and CA1-CA3 regions as defined for the main segmentation and analysis of variance
(CA: Cornu Ammonis; DG: Dentate Gyrus)

High field (14T) MRI was used at microscopy-level resolution to quantify R_2 and R_2* in subfields of the human hippocampus from Alzheimer's (AD) and control cases.

Mono-exponential Paravision fits of multi-gradient-echo and multi-spin multi-echo decays to obtain R2* and R2

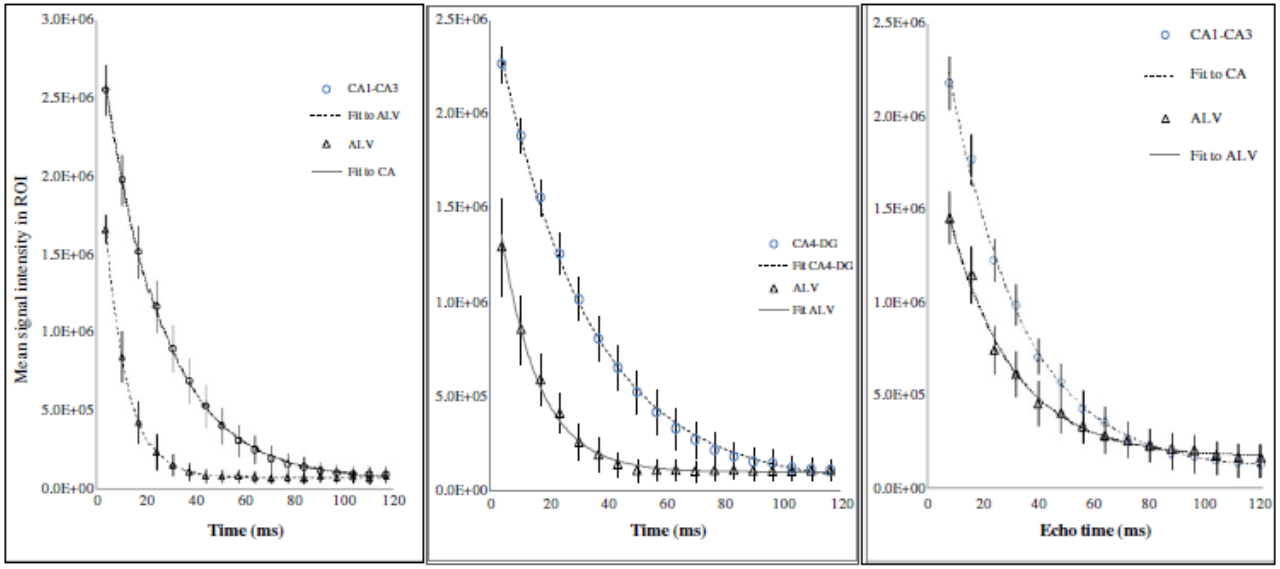

Multi-gradient-echo, case AD1, fixed tissue | Multi-gradient-echo, case C2, unfixed tissue | Multi-spin multi-echo, case AD1, fixed tissue

V. Antharam, J. F. Collingwood, et al. (2012) Neuroimage 59(2): 1249-1260.

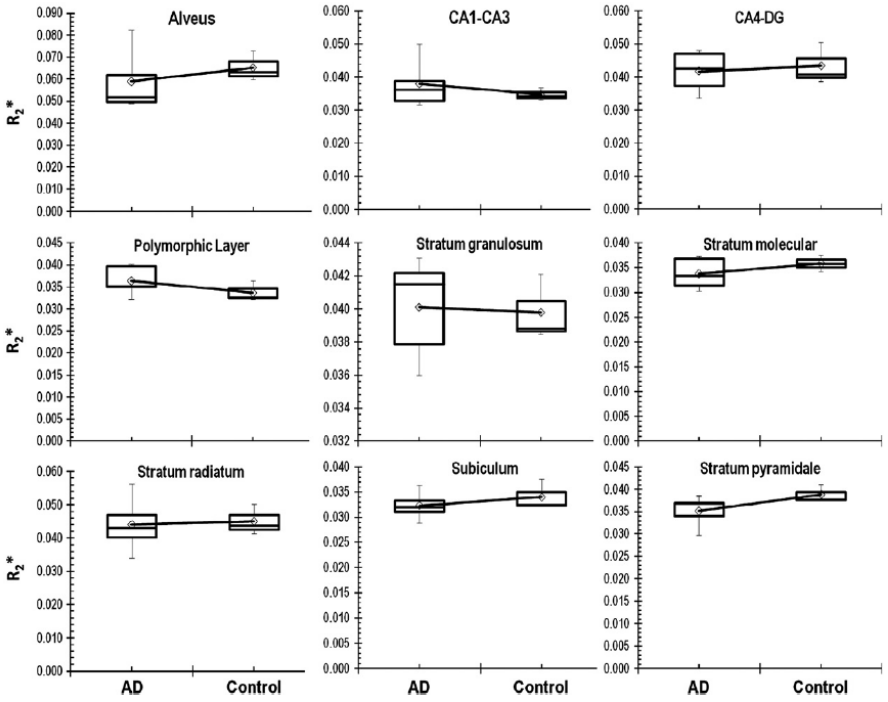

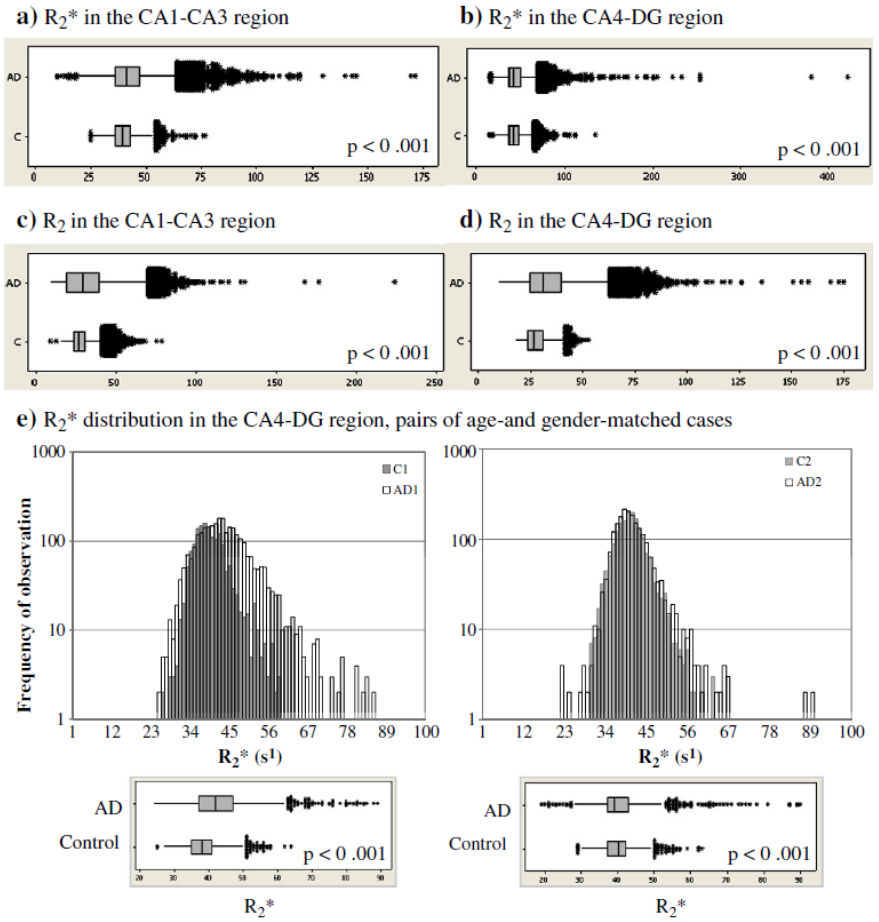

Fresh-frozen tissues:

- Magnitude of R_2 and R_2* changes very little for AD vs. control in segmented regions of HP.
- Variance in the Cornu Ammonis and dentate gyrus significantly higher in AD c.f. control ($p<0.001$).
- R_1 values consistently decreased in AD c.f. controls, ($p= 0.01$).

Fixed: Easier to prepare; average R_2 and R_2* values increased in AD fixed sample compared for the control (R_2* = 84 s^{-1} versus 35 s^{-1} in the CA1–CA3 region; 89 s^{-1} vs 38 s^{-1} in CA4–DG).

- R_2 and R_2* values give rise to good contrast, but absolute values not as consistent as in frozen.

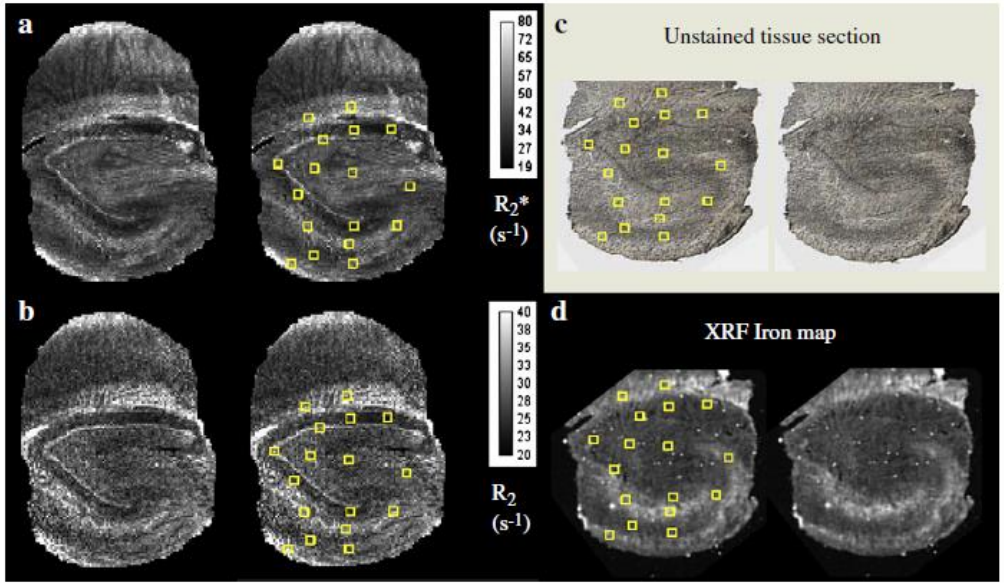

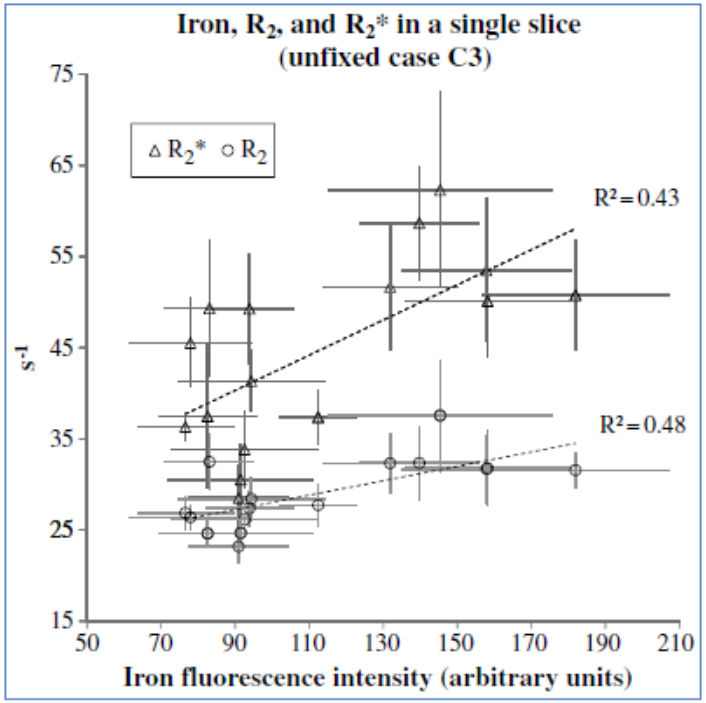

To investigate the relationship between tissue iron and MRI parameters, each tissue block was cryosectioned at 30 μm in the imaging plane.

Iron distribution was mapped using synchrotron microfocus X-ray fluorescence spectroscopy.

A positive correlation of R_2 and R_2* with iron was demonstrated.

V. Antharam, J. F. Collingwood, et al. (2012) Neuroimage 59(2): 1249-1260.

Q. Are changing patterns of brain iron deposition unique to each disease?

Comparison of tissues from Parkinson's disease, Multiple System Atrophy, and healthy controls.

3 healthy brains	(63 ± 23 yrs,	1 female, 2 males)
3 PD	(69 ± 12 yrs,	1 female, 2 males)
3 MSA	(63 ± 15 yrs,	1 female, 2 males)

Substantia nigra, basis pontis, putamen. All tissues frozen (i.e. not chemically fixed); all samples from the Canadian Brain Tissue Bank.

Identification of anatomical regions and subsequent dissection guided by Lili-Naz Hazrati (MD, PhD), Tanz Centre for Research in Neurodegenerative Disease, University of Toronto, Canada

Isothermal remanent magnetisation (IRM)

REVIEW OF SCIENTIFIC INSTRUMENTS 76, 045101 (2005)

Superconducting quantum interference device measurements of dilute magnetic materials in biological samples

D. Hautot[a)]
Institute for Science and Technology in Medicine, Keele University, Thornburrow Drive, Hartshill, Stoke-en-Trent, ST4 7QB, United Kingdom and London Centre for Nanotechnology and Department of Physics and Astronomy, University College London, Brook House, 2-16 Torrington Place, WC1E 7HN, United Kingdom

Q. A. Pankhurst
London Centre for Nanotechnology and Department of Physics and Astronomy, University College London, Brook House, 2-16 Torrington Place, WC1E 7HN, United Kingdom

J. Dobson
Institute for Science and Technology in Medicine, Keele University, Thornburrow Drive, Hartshill, Stoke-en-Trent, ST4 7QB, United Kingdom

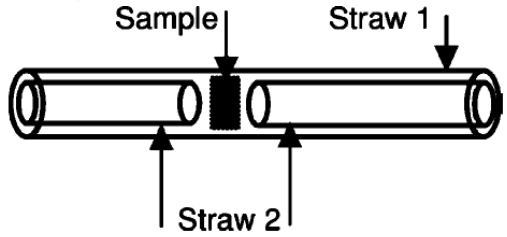

Biochim Biophys Acta. 2007 January ; 1772(1): 21–25.

Preliminary observation of elevated levels of nanocrystalline iron oxide in the basal ganglia of neuroferritinopathy patients

Dimitri Hautot[a], Quentin A. Pankhurst[b], Chris M. Morris[c,*], Andrew Curtis[d], John Burn[d], and Jon Dobson[a]

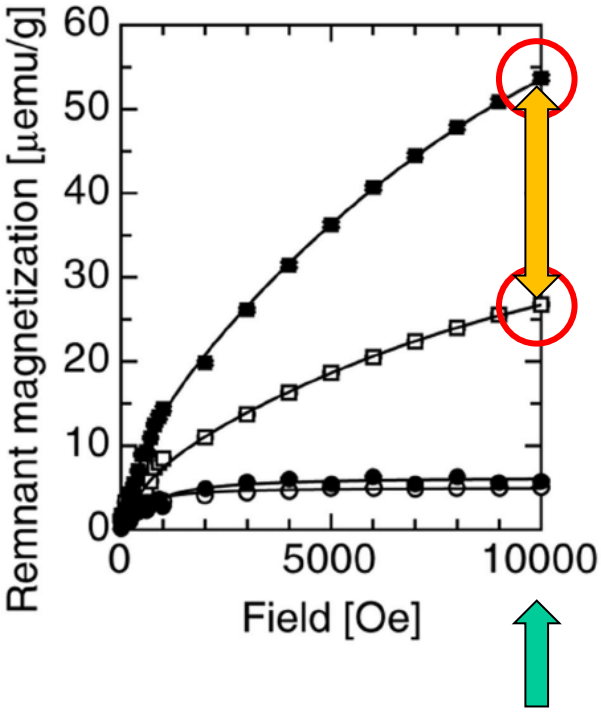

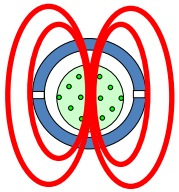

‘Blocked’
(5 K)

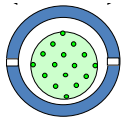

‘Unblocked’
(50 K)

IRM measurement at 1 Tesla,
at 5 K, 50 K and above.

Total iron | IRM @ 5 K | IRM vs iron

Basis pontis

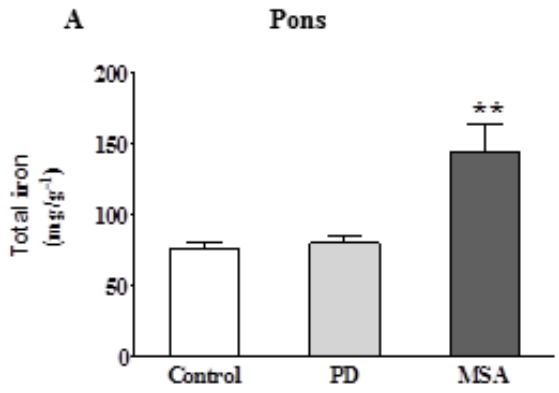

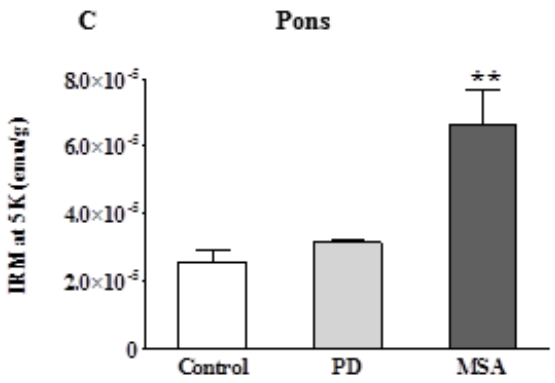

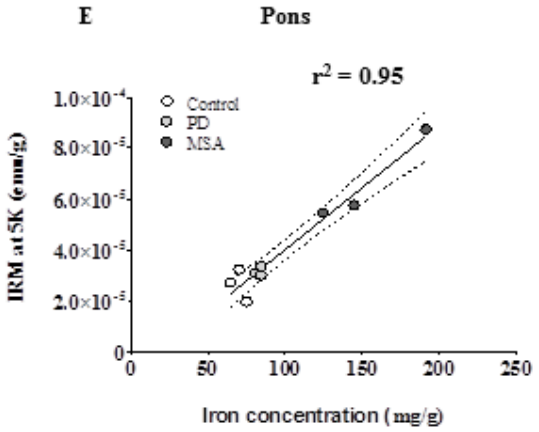

Substantia nigra

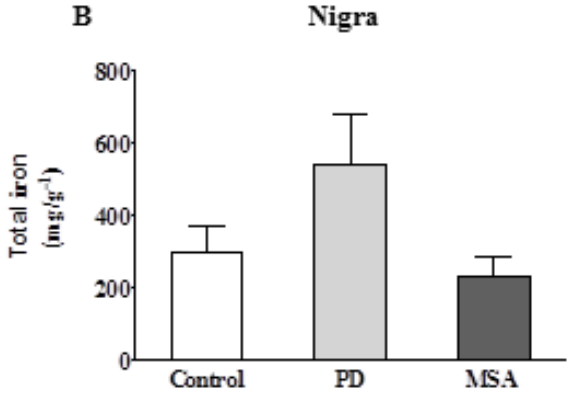

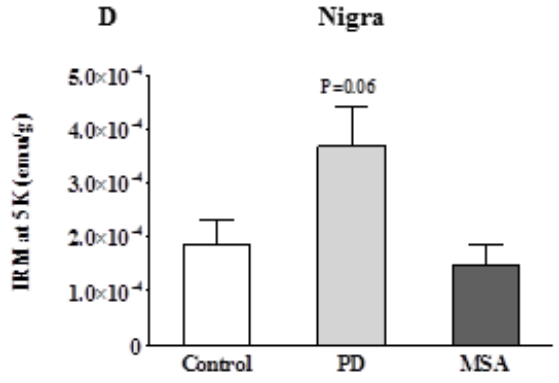

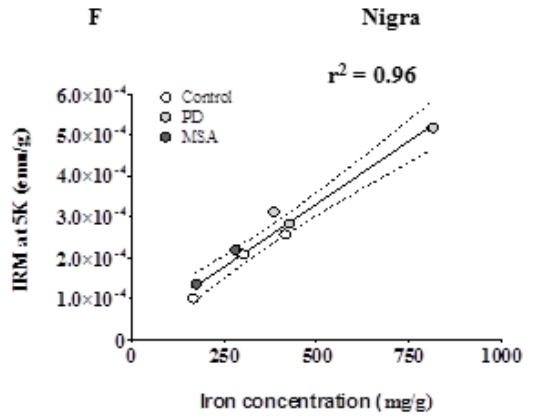

Total iron | Ferritin | Ferroportin

Basis pontis

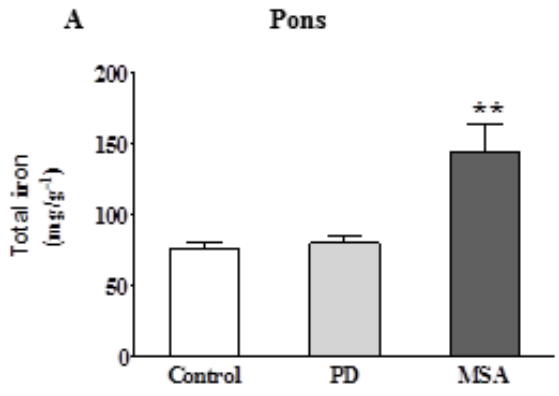

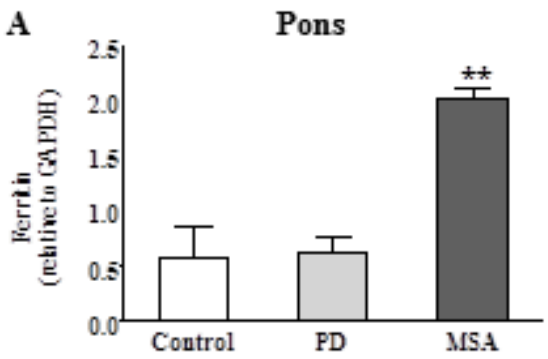

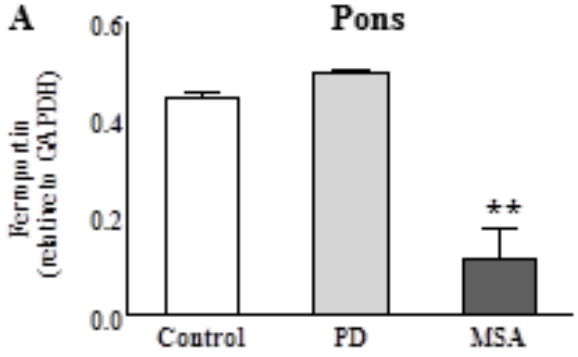

Substantia nigra

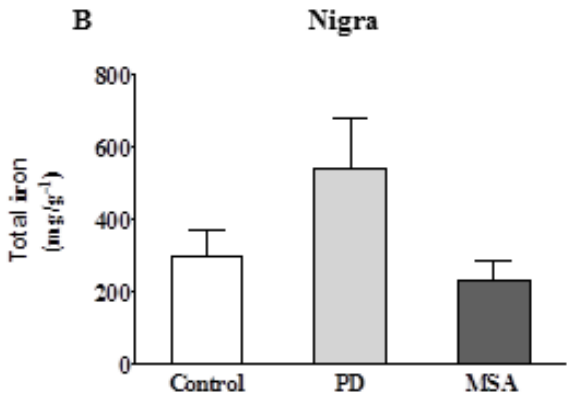

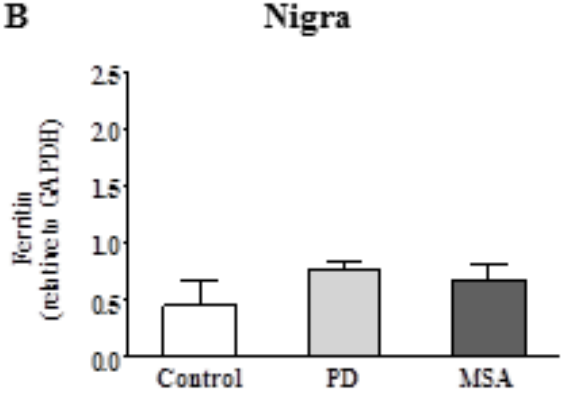

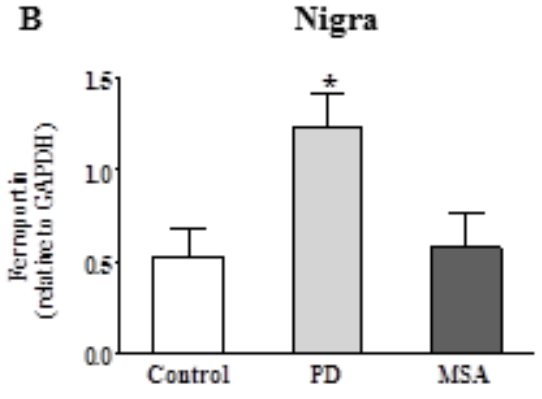

Visanji, Collingwood et al, accepted, Journal of Parkinson's Disease (2013)

WARWICK

Q. Are changing patterns of brain iron regulation and deposition unique to each disease?

	ALLOCATED GROUP	TRUE GROUP Control	MSA	PD
Ferritin	Control	**3**	0	0
100% success	MSA	0	**3**	0
	PD	0	0	**2**
Ferroportin	Control	**3**	0	0
100% success	MSA	0	**3**	0
	PD	0	0	**2**
Total iron	Control	**2**	0	0
88% success	MSA	0	**3**	0
	PD	(1)	0	**2**
Particulate iron (IRM @ 5K)	Control	**3**	0	0
100% success	MSA	0	**3**	0
	PD	0	0	**2**

Linear Discriminant Analysis (variables: basis pontis, substantia nigra, putamen)

Summary

- Developed methods to test relationship between structural MRI parameters (e.g. R_2, R_2*), iron concentration and distribution in unfixed brain tissue.

- Initial results from this small set of cases are consistent with
  i) Disease specificity in regional patterns of iron deposition
  ii) Disease specificity in modes of iron dysregulation

- These data are post-mortem. It is critical to determine at what point in the disease process iron dysregulation occurs.

ACKNOWLEDGEMENTS

Mary Finnegan, Martin Lees	UNIVERSITY OF WARWICK
Chris Exley, Emily House	KEELE UNIVERSITY
Mark Davidson, Jon Dobson	UNIVERSITY OF FLORIDA
Vijay Antharam, Saurav Chandra	
Chris Batich, John Forder,	
Albina Mikhailova	
Joe Gallagher	CALIFORNIA INSTITUTE OF TECHNOLOGY
Naomi Visanji and Lili Naz-Hazrati	TANZ CENTRE, UNIVERSITY OF TORONTO
Fred Mosselmans	DIAMOND
Paul Quinn, Tina Geraki	
Jeff Terry	IIT & MRCAT, APS
Soma Chaddopadhyay	MRCAT, APS
Marta Ugarte	UNIVERSITY OF MANCHESTER

With Thanks to Birmingham Science City Translational Medicine, Experimental Medicine Network of Excellence Project

WARWICK